frontiers in Astronomy and Space Sciences

ORIGINAL RESEARCH
published: 20 January 2022
doi: 10.3389/fspas.2021.802297

# Gas-Phase Reactivity of OH Radicals With Ammonia ($NH_3$) and Methylamine ($CH_3NH_2$) at Around 22 K

*Daniel González*[1], *Bernabé Ballesteros*[1,2], *André Canosa*[3], *José Albaladejo*[1,2] *and Elena Jiménez*[1,2]*

[1]Departamento de Química Física, Facultad de Ciencias y Tecnologías Químicas, Universidad de Castilla-La Mancha (UCLM), Ciudad Real, Spain, [2]Instituto de Investigación en Combustión y Contaminación Atmosférica, UCLM, Ciudad Real, Spain, [3]Institut de Physique de Rennes-CNRS—UMR 6251, Université de Rennes, Rennes, France

Interstellar molecules containing N atoms, such as ammonia ($NH_3$) and methylamine ($CH_3NH_2$), could be potential precursors of amino acids like the simplest one, glycine ($NH_2CH_2COOH$). The gas-phase reactivity of these N-bearing species with OH radicals, ubiquitous in the interstellar medium, is not known at temperatures of cold dark molecular clouds. In this work, we present the first kinetic study of these OH-reactions at around 22 K and different gas densities [(3.4–16.7) × $10^{16}$ $cm^{-3}$] in helium. The obtained rate coefficients, with ± 2σ uncertainties, can be included in pure gas-phase or gas-grain astrochemical models to interpret the observed abundances of $NH_3$ and $CH_3NH_2$. We observed an increase of $k_1$ and $k_2$ with respect to those previously measured by others at the lowest temperatures for which rate coefficients are presently available: 230 and 299 K, respectively. This increase is about 380 times for $NH_3$ and 20 times for $CH_3NH_2$. Although the OH + $NH_3$ reaction is included in astrochemical kinetic databases, the recommended temperature dependence for $k_1$ is based on kinetic studies at temperatures above 200 K. However, the OH + $CH_3NH_2$ reaction is not included in astrochemical networks. The observed increase in $k_1$ at ca. 22 K does not significantly change the abundance of $NH_3$ in a typical cold dark interstellar cloud. However, the inclusion of $k_2$ at ca. 22 K, not considered in astrochemical networks, indicates that the contribution of this destruction route for $CH_3NH_2$ is not negligible, accounting for 1/3 of the assumed main depletion route (reaction with $HCO^+$) in this IS environment.

$$k_1\,(\mathrm{OH} + \mathrm{NH_3}) = (2.7 \pm 0.1) \times 10^{-11}\mathrm{cm^3 s^{-1}}$$
$$k_2\,(\mathrm{OH} + \mathrm{CH_3NH_2}) = (3.9 \pm 0.1) \times 10^{-10}\mathrm{cm^3 s^{-1}}$$

**Keywords: ISM, prebiotic molecules, OH radicals, CRESU technique, reaction kinetics, ultralow temperatures**

OPEN ACCESS

***Edited by:***
*Majdi Hochlaf,*
*Université Paris Est Marne la Vallée, France*

***Reviewed by:***
*Marzio Rosi,*
*University of Perugia, Italy*
*Christian Alcaraz,*
*Centre National de la Recherche Scientifique (CNRS), France*

***Correspondence:**
*Elena Jiménez*
*Elena.Jimenez@uclm.es*

***Specialty section:***
*This article was submitted to Astrochemistry, a section of the journal Frontiers in Astronomy and Space Sciences*

***Received:*** *26 October 2021*
***Accepted:*** *02 December 2021*
***Published:*** *20 January 2022*

***Citation:***
*González D, Ballesteros B, Canosa A, Albaladejo J and Jiménez E (2022) Gas-Phase Reactivity of OH Radicals With Ammonia ($NH_3$) and Methylamine ($CH_3NH_2$) at Around 22 K. Front. Astron. Space Sci. 8:802297. doi: 10.3389/fspas.2021.802297*

## INTRODUCTION

Unravelling the origin of life on the Earth has been both a challenge and a matter of debate for scientists throughout the history. However, what we can be certain about is that all ingredients essential for life are composed by a few atoms such as H, O, C, N, or S. The combination of these atoms can produce different prebiotic molecules, which are considered the precursors of life on our

planet. Principally, two main theories have been proposed for trying to explain how these molecules could have appeared on the globe (Chyba and Sagan, 1992; Bernstein, 2006). The first one states that the organic molecules that serve as the basis of life were formed in the primitive atmosphere of our planet from simpler and smaller molecules (e.g., $NH_3$, $CH_4$, $H_2O$, or $H_2$) (Miller, 1953; Bada and Lazcano, 2002; Cleaves et al., 2008). In fact, this was demonstrated experimentally by Stanley Miller in the middle of the past century when he obtained a considerable number of important compounds from the biological point of view, such as amino acids, from simple molecules like the aforementioned, after exposing them to conditions aiming at mimicking those reigning in the primitive Earth (Miller, 1953). The second one is based on the idea that the prebiotic molecules were firstly synthesized in space and then, they could have been delivered to the Earth by meteorites, comets, asteroids or even interplanetary dust particles (Ehrenfreund et al., 2002; Sandford et al., 2020). This latter hypothesis is now in trend due to the huge and unexpected discovery in the last 70 years of the chemical richness in the interstellar medium (ISM). Currently, about 250 species (including ions and neutrals) have been detected in the ISM or circumstellar shells (Woon, 2021). Interstellar molecules, which are found in ultra-cold environments (~10–100 K), such as the so-called dense or dark clouds or pre-stellar cores, range from simple diatomic molecules [e.g., CO or the hydroxyl (OH) radical] to more complex systems (e.g., fullerenes). For instance, the OH radical, firstly detected in Cassiopeia A in 1963 (Weinreb et al., 1963), is ubiquitous in the ISM. By definition, carbon-bearing species containing six atoms or more are called complex organic molecules (COMs) (Herbst and van Dishoeck, 2009). Some COMs containing C-O bonds (such as $CH_3OH$) and C-N bonds (such as $CH_3CN$) can be potential precursors of sugars and amino acids in the presence of water, respectively (Balucani, 2009), under the Earth's conditions. Although ammonia ($NH_3$) is not considered a COM, strictly by definition, this abundant nitrogen-bearing species is very important since it serves as temperature probe in molecular clouds like Sagittarius (Sgr) B2, where it was first detected (Cheung et al., 1968). Ammonia has also been found towards a post-star forming region, W3(OH), with an abundance relative to $H_2$ of $10^{-8}$ (Wilson et al., 1993) and in TMC-1, with a column density of $\sim 10^{15}\,cm^{-2}$ (Freeman and Millar, 1983). Another interesting N-bearing species is methylamine ($CH_3NH_2$), which was detected in the 1970s years for the first time towards Sgr B2 and Orion A (Fourikis et al., 1974; Kaifu et al., 1974). Abundances relative to $H_2$ for $CH_3NH_2$ have been observed to be $10^{-8}$ towards the hot core G10.47 + 0.33 (Ohishi et al., 2019) and $10^{-9}$ for Sgr B2 (Halfen et al., 2013). Both $NH_3$ and $CH_3NH_2$ have been proposed as precursors of the simplest amino acid, glycine ($NH_2CH_2COOH$), through H-atom abstraction reactions forming $NH_2$ (Sorrell, 2001; Garrod, 2013) and $CH_2NH_2$ radicals, (Woon, 2002; Garrod, 2013); however interstellar glycine remains undetected in the ISM so far.

Under the ISM conditions, it has been assumed since a long time (Herbst and Klemperer, 1973) that dissociative recombination of $NH_4^+$ is the main provider of $NH_3$ in the gas phase. This cation can be generated through a series of hydrogen abstraction reactions starting from $N^+ + H_2$ leading step by step to $NH^+$, $NH_2^+$, $NH_3^+$, and eventually $NH_4^+$ (Gerin et al., 2016; Rednyk et al., 2019). Alternatively, $NH_2^+$ can be produced by $H_3^+ + N$ (Scott et al., 1997). Although not included in interstellar chemical networks, another potential source of $NH_3$ was recently claimed by Gianturco et al. (2019) to be the reaction of the $NH_2^-$ anion with $H_2$. Surface reactions have also been proposed as plausible mechanisms to produce ammonia via a series of atomic hydrogen additions to N-hydrides after NH has been formed through N + H → NH (Jonusas et al., 2020). Regarding $CH_3NH_2$, different synthetic routes have been proposed. In the gas-phase, it may be formed via the radiative association between $NH_3$ and the methyl radical cation ($CH_3^+$) followed by dissociative recombination (Herbst, 1985). But $CH_3NH_2$ can also be formed on grain surfaces by sequential hydrogenation of hydrogen cyanide (HCN), as experimentally observed by Theule et al. (2011). Simulations of the irradiation of $CH_4$ and $NH_3$ ices may also form $CH_3NH_2$ (Kim and Kaiser, 2011; Förstel et al., 2017), but also in cold and quiescent molecular clouds (Ioppolo et al., 2021). In the gas-grain chemical model by (Garrod et al., 2008), the $CH_3$+$NH_2$ reaction was also suggested as a source of $CH_3NH_2$ during warm-up phases.

It is also important to know how $NH_3$ and $CH_3NH_2$ are being destroyed to have a good insight of the chemical evolution of the ISM. Focusing on neutral-neutral reactions, reaction networks that astrochemical models used, such as KIDA and UDfA, include eight depletion routes for $NH_3$. e.g., reactions with H, CH, CN, among other radicals. Concerning $CH_3NH_2$, only two depleting reactions by CH and $CH_3$ radicals are included in KIDA database, while UDfA database does not include any. Until now, the reactivity of $NH_3$ with neutral radicals or atoms at ISM temperatures has been investigated experimentally in the presence of CN (Sims et al., 1994), CH (Bocherel et al., 1996), $C_2H$ (Nizamov and Leone, 2004) and $C(^3P)$ (Bourgalais et al., 2015; Hickson et al., 2015) whereas, only the reactivity of $CH_3NH_2$ with CN is documented (Sleiman et al., 2018a; 2018b). Due to the important role of OH radicals as a key intermediate in multiple reactive processes in the ISM (Cazaux et al., 2010; Goicoechea et al., 2011; Acharyya et al., 2015; Linnartz et al., 2015), the kinetic database for OH-molecule reactions has been widely extended in the past years (see e.g., Taylor et al., 2008; Smith and Barnes, 2013; Ocaña et al., 2017, 2019; Potapov et al., 2017; Heard, 2018; Blázquez et al., 2019, 2020). For the OH + $NH_3$ reaction (**Eq. R1**), of interest in atmospheric and combustion chemistry, its gas-phase kinetics has been extensively studied both experimentally and theoretically.

$$OH + NH_3 \rightarrow H_2O + NH_2 \qquad k_1 \qquad (R1)$$

Note that other reaction channels forming $H_2NO + H_2$, $HNOH + H_2$, or $H_2NOH + H$ are not thermodynamically accessible, since they are endothermic by Gibbs free energies ranging from 19.67 to 31.73 kcal/mol (Vahedpour et al., 2018). **Eq. R1** is also of astrochemical interest since it leads to the formation of $NH_2$ radicals, which were also observed towards the same location as ammonia (van Dishoeck et al., 1993). In the laboratory studies, the

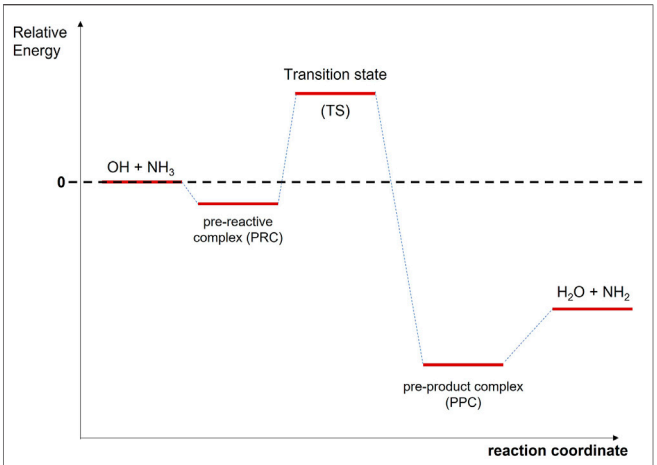


**SCHEME 1 |** Simplified reaction energy profile along the MEP for the OH + $NH_3$ reaction.

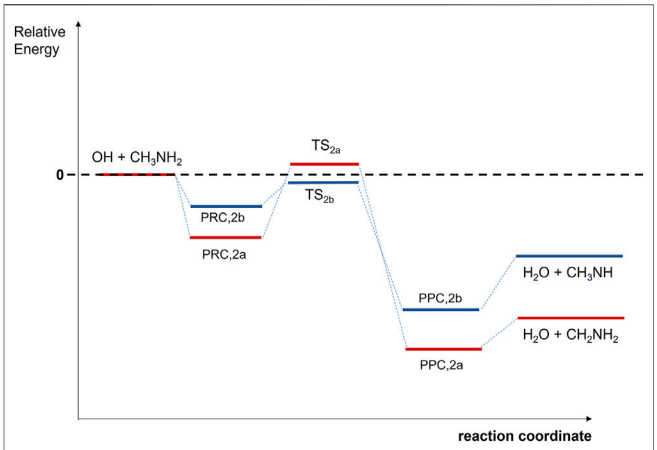


**SCHEME 2 |** Simplified reaction energy profile along the MEP for the OH + $CH_3NH_2$ reaction.

rate coefficient for R1, $k_1$, has been reported since the 1970's by many research groups over a wide range of temperature (230–2,360 K) and pressures (1–4,000 mbar) (Stuhl, 1973; Kurylo, 1973; Zellner and Smith, 1974; Hack et al., 1974; Perry et al., 1976; Silver and Kolb, 1980; Fujii et al., 1981, 1986; Salimian et al., 1984; Stephens, 1984; Zabielski and Seery, 1985; Jeffries and Smith, 1986; Diau et al., 1990). A summary of all previous experimental results can be found in Diau et al. (1990). The observed dependence of $k_1$ with temperature is positive, i.e., the rate coefficient increases when temperature increases, and the reported activation energies range from 0.5 to 9 kcal/mol in the 230–2,360 K range (Zellner and Smith, 1974; Hack et al., 1974; Perry et al., 1976; Silver and Kolb, 1980; Fujii et al., 1981, 1986; Salimian et al., 1984; Stephens, 1984; Zabielski and Seery, 1985; Jeffries and Smith, 1986; Diau et al., 1990). The computed energy barriers in the 200–4,000 K range were found to be between 2.0 and 9.05 kcal/mol (Giménez et al., 1992; Corchado et al., 1995; Bowdridge et al., 1996; Nyman, 1996; Lynch et al., 2000; Monge-Palacios et al., 2013b; Nguyen and Stanton, 2017). The reaction mechanism of R1 was also theoretically investigated (Giménez et al., 1992; Espinosa-García and Corchado, 1994; Corchado et al., 1995; Bowdridge et al., 1996; Nyman, 1996; Lynch et al., 2000; Monge-Palacios et al., 2013b; Nguyen and Stanton, 2017). The formation of a pre-reactive complex (PRC) at the entrance channel is accepted, as illustrated in **Scheme 1**, and quantum mechanical tunneling has been reported to be an important contribution to $k_1$, leading to the observed non-Arrhenius behavior (Espinosa-García and Corchado, 1994; Corchado et al., 1995; Bowdridge et al., 1996; Nyman, 1996; Monge-Palacios et al., 2013b; Nguyen and Stanton, 2017).

Regarding the OH + $CH_3NH_2$ reaction (**Eq. R2**), previous kinetic studies are restricted to temperatures higher than 295 K (Atkinson et al., 1977; Carl and Crowley, 1998; Onel et al., 2013; Butkovskaya and Setser, 2016). From the experimental point of view, Atkinson et al. (1977), Onel et al. (2013) reported the temperature dependence of reaction R2 in the 299–426 K and 298–600 K ranges, respectively. A negative temperature dependence of $k_2$ was observed and this rate coefficient increases when temperature decreases.

$$OH + CH_3NH_2 \rightarrow \text{products} \qquad k_2 \qquad \text{(R2)}$$

**Eq. R2** may proceed by H-abstraction from methyl (–$CH_3$) or amino (–$NH_2$) groups forming $CH_2NH_2$ and $CH_3NH$ radicals plus water, respectively. The formation of $CH_2NH_2$ radicals was measured to be the main reaction channel at room temperature (Nielsen et al., 2011, 2012; Onel et al., 2014; Butkovskaya and Setser, 2016), in agreement with theoretical predictions at 299 K and above (Galano and Alvarez-Idaboy, 2008; Tian et al., 2009). These calculations suggest a stepwise mechanism involving the formation of a PRC at the entrance channels and an energy barrier of a few kcal/mol for the H-abstraction channel from –$CH_3$ group, as depicted in **Scheme 2**.

As there are no kinetic data of $k_1$ and $k_2$ at temperatures of the cold dark interstellar clouds and since they are necessary to properly model the chemistry of the ISM, we present in this work the first determination of the rate coefficient for the reactions of $NH_3$ and $CH_3NH_2$, $k_i$ ($i$ = 1 or 2), with OH radicals at ca. 22 K using a combination of a pulsed CRESU (French acronym for Reaction Kinetics in a Uniform Supersonic Flow) reactor with laser techniques. The implications of the reported new rate coefficients will be discussed in terms of their effect on the predicted abundances of $NH_3$ and $CH_3NH_2$ in a typical cold dark interstellar cloud at 10 K.

## EXPERIMENTAL METHODS

### CRESU Apparatus Coupled to Pulsed Laser Photolysis-Laser Induced Fluorescence Technique

The experimental system based on the pulsed uniform supersonic expansion of a gas mixture has been already described elsewhere (Jiménez et al., 2015, 2016; Antiñolo et al., 2016; Canosa et al., 2016; Ocaña et al., 2017, 2018, 2019; Blázquez et al., 2019, 2020; Neeman et al., 2021). To carry out the kinetic experiments, three Laval nozzles (He23-HP, He23-IP, and He23-LP) were used with

**TABLE 1 |** Summary of the experimental conditions [total gas density (*n*), jet pressure (*p*), and reactant concentration in the jet] and corrected *pseudo*-first order rate coefficient ranges.

| Reactant | Laval nozzle | $n/10^{16}$ cm$^{-3}$ | *p*/mbar | [Reactant]/$10^{13}$ cm$^{-3}$ | $k'$-$k'_0$/s$^{-1}$ | $k$(T) /$10^{-11}$ cm$^3$ s$^{-1}$ |
|---|---|---|---|---|---|---|
| $NH_3$ | He23-HP | 16.7 | 0.51 | 4.2–21.6 | 1932–5613 | 2.7 ± 0.1 |
| | He23-IP | 7.4 | 0.23 | 3.5–10.7 | 1177–2737 | 2.7 ± 0.1 |
| | He23-LP | 3.4 | 0.10 | 2.9–8.6 | 408–2886 | 2.9 ± 0.3 |
| $CH_3NH_2$ | He23-HP | 16.7 | 0.51 | 0.3–3.1 | 589–11713 | 39.2 ± 2.0 |
| | He23-IP | 7.4 | 0.23 | 0.7–3.1 | 3317–11166 | 36.2 ± 1.4 |
| | He23-LP | 3.4 | 0.10 | 0.6–2.9 | 2382–12034 | 41.1 ± 1.5 |

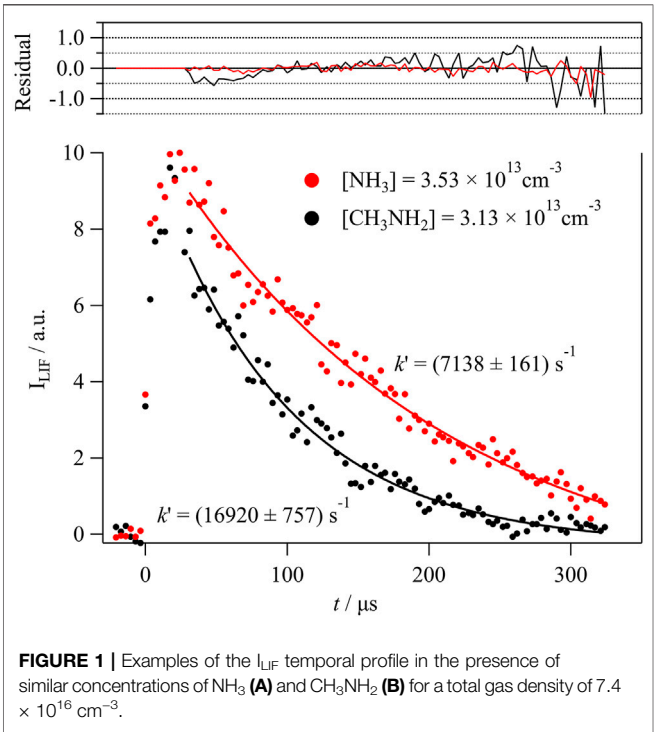


**FIGURE 1 |** Examples of the $I_{LIF}$ temporal profile in the presence of similar concentrations of $NH_3$ **(A)** and $CH_3NH_2$ **(B)** for a total gas density of 7.4 × $10^{16}$ cm$^{-3}$.

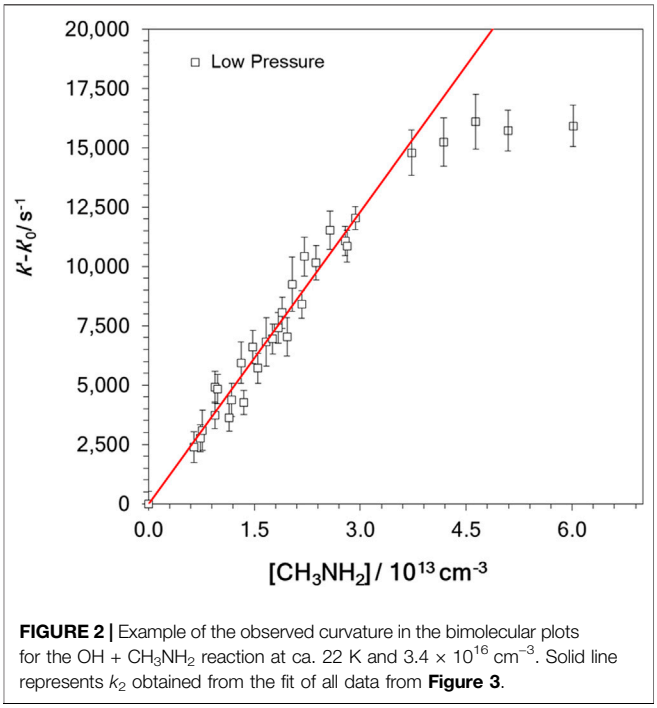


**FIGURE 2 |** Example of the observed curvature in the bimolecular plots for the OH + $CH_3NH_2$ reaction at ca. 22 K and 3.4 × $10^{16}$ cm$^{-3}$. Solid line represents $k_2$ obtained from the fit of all data from **Figure 3**.

helium as a carrier gas. These nozzles were designed to generate a uniform flow at around 22 K for three different jet pressures (see **Table 1**) (Jiménez et al., 2015; Canosa et al., 2016; Ocaña et al., 2017), thus allowing us to explore the influence of pressure on the reactivity at a constant temperature. Bath gas and reactants ($NH_3$ or $CH_3NH_2$) were introduced in the CRESU chamber through calibrated mass flow controllers, MFCs (Sierra Instruments, Inc., model Smart Trak, Smart-Trak 2, MicroTrak 101, and Smart-Trak 100). $CH_3NH_2$ was diluted in He and stored in a 20-L or 50-L bulb. Calibrated mass flow rates of these diluted mixtures ranged from 6.6 to 200 sccm (standard cubic centimeters per minute), depending on the Laval nozzle used. Dilution factor *f* ranged from 1.78 × $10^{-2}$ to 4.54 × $10^{-2}$. In contrast, $NH_3$ was flown directly to the pre-expansion chamber (reservoir) from a gas cylinder through a MFC manufactured with anticorrosive materials (Sierra Instruments, Inc., model Smart-Trak 100). The flow rates of pure $NH_3$ ranged from 3 to 15 sccm. The OH-precursor employed was $H_2O_2$, since it is a clean source of OH radicals. Gaseous $H_2O_2$ was introduced into the reservoir by bubbling the bath gas through an aqueous solution of $H_2O_2$, as explained in Jiménez et al. (2005). The flow rate of He through the $H_2O_2$ bubbler in different experiments ranged from 35.6 to 265.8 sccm, depending on the Laval nozzle used. Within a kinetic experiment, this flow rate was kept constant to maintain invariable the contribution of the OH loss due to the OH + $H_2O_2$ reaction (see Kinetic *Analysis*). The gas mixture formed by He (main flow), He/$H_2O_2$, and the reactant was pulsed by a two holes rotary disk described in Jiménez et al. (2015).

After the gas expansion through the Laval nozzle, the jet temperature was measured by a Pitot tube to be (21.7 ± 1.4) K for the He23-HP nozzle, (22.5 ± 0.7) K for the He23-IP nozzle, and (21.1 ± 0.6) K for the He-23LP nozzle, respectively. Within the fluctuation along the flow axis (± σ), the jet temperature in all cases is ca. 22 K. The procedure to determine the jet temperature and gas density has been previously described (Jiménez et al., 2015; Canosa et al., 2016; Ocaña et al., 2017). Pulsed photolysis of $H_2O_2$(g) at 248 nm was achieved by the radiation coming from a KrF excimer laser (Coherent, model ExciStar XS 200) with energies at the exit of the nozzle ranging from 0.5 to 0.9 mJ/pulse at 10 Hz, depending on the nozzle used. OH radicals were monitored by collecting the laser induced fluorescence (LIF) at

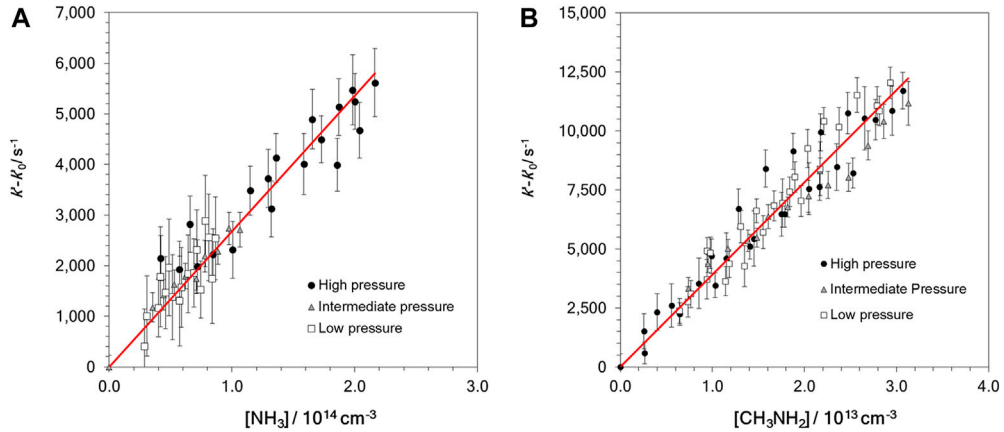


**FIGURE 3 |** Bimolecular plots for the OH-reactions at ca. 22 K with **(A)** $NH_3$ and **(B)** $CH_3NH_2$.

310 nm, after laser excitation at *ca.* 282 nm, as a function of the reaction time defined as the time delay between the probe laser pulse and the excimer one.

## Kinetic Analysis

In **Figure 1** an example of the temporal evolution of the LIF intensity ($I_{LIF}$) is presented. As explained in several papers (Jiménez et al., 2015; Ocaña et al., 2018), the observed rise of the $I_{LIF}$ signal at $t > 0$ is due to rotational relaxation of OH, coming from $H_2O_2$ photodissociation, that occurs in a timescale ($t_0$) of less than 30 μs under the conditions of the experiments, especially, at the concentration levels of the reactant, which is an effective quencher. The fit of the recorded $I_{LIF}$ profiles to an exponential decay (solid lines in **Figure 1**) confirms that the OH loss follows a pseudo-first order kinetics.

$$\boldsymbol{I_{LIF}(t) = I_{LIF}(t_0)\, exp^{-k'(t-t_0)}} \quad \text{(E1)}$$

The pseudo-first order rate coefficient, $k'$, includes all the OH loss processes occurring simultaneously in the cold jet.

$$\boldsymbol{k' = k'_0 + k_i[Reactant]} \quad \text{(E2)}$$

where $k_i$ ($i$ = 1 or 2) is the bimolecular rate coefficients for OH-reactions with $NH_3$ (R1) and $CH_3NH_2$ (R2). In the absence of reactant, $k'_0$ was measured, and it included the loss of OH radicals by OH-reaction with $H_2O_2$ and other OH losses, such as diffusion out of the detection zone. In **Table 1**, the ranges of the employed reactant concentration, [Reactant], and the determined $k'$–$k'_0$ values are summarized. According to **Eq. E2**, the slopes of the $k'$-$k'_0$ *versus* [Reactant] plots yield the bimolecular rate coefficients $k_i$. Nevertheless, the linear relationship between $k'$-$k'_0$ and [Reactant] is not always accomplished, as shown in the example in **Figure 2**. In this figure, a downward curvature in the plot of $k'$-$k'_0$ vs. $[CH_3NH_2]$ was observed at concentrations higher than $3 \times 10^{13}$ $cm^{-3}$. As discussed in previous works (Ocaña et al., 2017, 2019; Blázquez et al., 2020; Neeman et al., 2021), this curvature may be the result of the dimerization of the OH-co reactant, $CH_3NH_2$ in this case. Considering the onset of dimerization, the red straight line in **Figure 2** represents the fit to **Eq. E2** at $[CH_3NH_2]$ below ~$3 \times 10^{13}$ $cm^{-3}$. In contrast, for reaction R1 the plot of $k'$-$k'_0$ vs. $[NH_3]$ is linear over the entire concentration range, as displayed in **Figure 3A**. Since this concentration range is much larger than the one for $CH_3NH_2$ and that the reactivity with OH is significantly slower for $NH_3$ than for $CH_3NH_2$, it shows that the dimerization of $NH_3$ is much less efficient than that of $CH_3NH_2$ at 22 K. In **Figure 3B**, all kinetic data obtained in the linear part of the $k'$-$k'_0$ vs. $[CH_3NH_2]$ plot are depicted. The bimolecular rate coefficient $k_2$ at ca. 22 K is, then, obtained from the slope of such a plot.

Reagents Gases: He (99.999%, Nippon gases), $NH_3$ (≥ 99.95%, Merck) and $CH_3NH_2$ (≥ 99.0%, Merck) were used as supplied. Aqueous solution of $H_2O_2$ (Sharlab, initially at 50% w/w) was pre-concentrated as explained earlier (Albaladejo et al., 2003).

# RESULTS AND DISCUSSION

## The OH + $NH_3$ Reaction

### Temperature Dependence of $k_1$

A summary of the individual rate coefficients $k_1$ obtained at 22 K and different total pressures of the gas jet is presented in **Table 1**. Within the stated statistical uncertainties (± 2σ), no pressure dependence of $k_1$ was observed in the investigated range (0.10–0.51 mbar). For this reason, we combined all the kinetic results, as shown in **Figure 3A** The resulting rate coefficient for the OH + $NH_3$ reaction at ca. 22 K is:

$$\boldsymbol{k_1(\sim 22\,K) = (2.27 \pm 0.1) \times 10^{-11} cm^3 s^{-1}}$$

where the uncertainty (± 2σ) only includes statistical errors. An additional 10% uncertainty has to be added to account for the systematic errors.

As mentioned in the Introduction section, **Eq. R1** has been investigated under extensive experimental conditions of temperature (230–2,360) K and pressure (1–4,000 mbar). A summary of all previous kinetic studies can be found in the most recent investigation from Diau et al. (1990). Focusing on the works carried out as a function of temperature (Zellner and

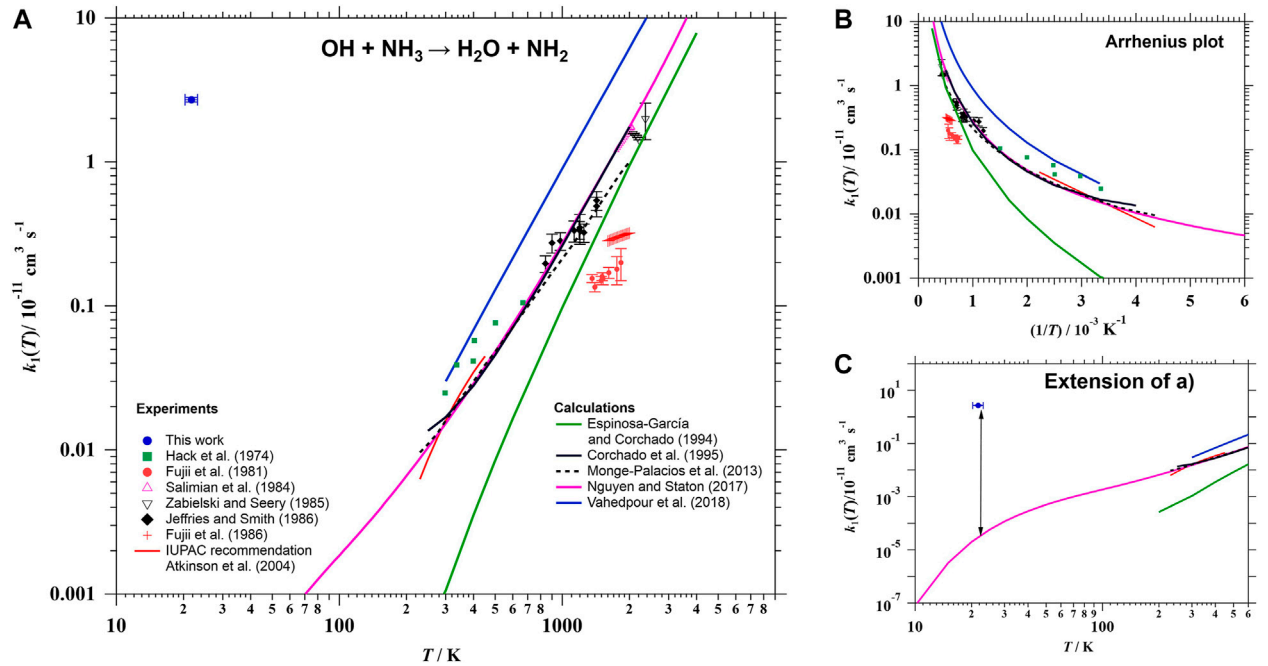


**FIGURE 4 | (A)** Temperature dependence of $k_1$ (log-log plot) in the 22–4,000 K range. Individual rate coefficients at room temperature K (Zellner and Smith, 1974; Perry et al., 1976; Silver and Kolb, 1980; Stephens, 1984; Diau et al., 1990) are not included in the figure, but they are considered in the IUPAC recommendation (red curve). **(B)** Arrhenius plot for $k_1$ between 170 and 4,000 K to better see the curvature (non-Arrhenius behavior). **(C)** Extension of the log-log plot shown in **(A)** to show the great enhancement of $k_1$ with respect to theoretical predictions at 20 K.

Smith, 1974; Hack et al., 1974; Perry et al., 1976; Silver and Kolb, 1980; Fujii et al., 1981, 1986; Salimian et al., 1984; Stephens, 1984; Zabielski and Seery, 1985; Jeffries and Smith, 1986; Diau et al., 1990), a positive temperature dependence of $k_1$ was observed in all cases, as shown in **Figure 4A**. For instance, IUPAC recommends a T-expression for $k_1$, based on previous results below 450 K (Zellner and Smith, 1974; Perry et al., 1976; Silver and Kolb, 1980; Stephens, 1984; Diau et al., 1990), with an $E_a$/R factor of 925 K which yields an activation energy ($E_a$) of 1.8 kcal/mol (Atkinson et al., 2004):

$$k_1\,(230-450\,K) = 3.5\times10^{-12}exp^{-925\ K/T}\ \ cm^3s^{-1} \qquad \text{(E3)}$$

Even so, as hydrogen atom transfer reactions usually show significant dynamical quantum effects (see Reaction mechanism), the kinetics of reaction R1 deviates from the Arrhenius behavior, showing a curvature in the plot of $ln\ k_1$ versus $1/T$. This deviation from Arrhenius behavior has been observed experimentally between 840 and 1,425 K (Jeffries and Smith, 1986) and predicted theoretically between 5 and 4,000 K (Espinosa-García and Corchado, 1994; Corchado et al., 1995; Monge-Palacios et al., 2013b; Nguyen and Stanton, 2017; Vahedpour et al., 2018). Most of the computed $k_1$ have been reported at temperatures higher than 200 K (Espinosa-García and Corchado, 1994; Corchado et al., 1995; Monge-Palacios et al., 2013b; Vahedpour et al., 2018). Only the calculations by Nguyen and Stanton (2017) were performed at lower temperatures and down to 5 K. For ease of presentation, kinetic data between 170 and 4,000 K are plotted in **Figure 4B** in Arrhenius form to clearly show the curvature. Down to 20 K, the predicted $k_1$ by Nguyen and Stanton (2017), represented by a pink line in **Figure 4C**, was $2\times10^{-16}$ cm$^3$ s$^{-1}$. This value is around five orders of magnitude lower than the experimental result reported in this work. Certainly, further kinetic studies between 230 and 22 K (and even below) are needed and are planned in our laboratory in the future.

## Reaction Mechanism

As stated in the Introduction section, the reaction mechanism of the OH + $NH_3$ reaction has been widely studied from a theoretical point of view. The effects of vibrational and translational energy of $NH_3$ and OH counter partners have been studied by quasi-classical trajectories (Nyman, 1996; Monge-Palacios and Espinosa-Garcia, 2013; Monge-Palacios et al., 2013a) and by quantum scattering calculations (Nyman, 1996). Besides these dynamical studies, *ab initio* calculations based on the transition state theory (TST) were reported. In **Scheme 1**, a simplified illustration of the relative energies to the reactants of the stationary points along the minimum energy pathway (MEP) for the OH + $NH_3$ system is shown. Some studies proposed that product formation in reaction R1 occurs from the transition state and reported energy barriers ranged from 2.03 kcal/mol to 8.94 kcal/mol (Giménez et al., 1992; Bowdridge et al., 1996; Lynch et al., 2000). However, other investigations proposed that reaction R1 occurs through a H-bonded PRC at the entrance channel (Corchado et al., 1995; Bowdridge et al.,

**TABLE 2 |** Summary of the calculated energies relative to reactants (in kcal/mol) of the stationary points in the MEP for the OH + $NH_3$ reaction reported in the literature (see text for more details).

| PRC | TS | PPC | Products | References |
|---|---|---|---|---|
| −1.75 | 8.94 | — | −10.69[a] | Giménez et al. (1992) |
| | 9.05 | −15.02 | −8.98 | Espinosa-García and Corchado (1994) |
| | 3.65 | −17.39 | −11.96 | Corchado et al. (1995) |
| | 2.03 | — | — | Bowdridge et al. (1996) |
| | 4.4 | — | −7.1 | Lynch et al. (2000) |
| −1.8 | 3.3 | −15.6 | −10.0 | Monge-Palacios et al. (2013b) |
| 0.33 | 2.6 | −14.47 | −11.49 | Nguyen and Stanton (2017) |

[a]From $\Delta H^{o}_{r298\ K}$.

1996; Monge-Palacios et al., 2013b; Nguyen and Stanton, 2017). The relative energy of this PRC is positioned a few kcal/mol above the reactants (Nguyen and Stanton, 2017) or −1.8 kcal/mol (Corchado et al., 1995; Monge-Palacios et al., 2013b). In addition to the PRC, a H-bonded complex near the products (PPC, pre-product complex) (Espinosa-García and Corchado, 1994; Corchado et al., 1995; Monge-Palacios et al., 2013b; Nguyen and Stanton, 2017) is proposed at the exit channel, which is stabilized with respect to the reactants by *ca.* −15 kcal/mol. **Table 2** summarizes the relative energies of PRC, TS, and PPC from theoretical calculations reported in the literature.

Note that the reaction pathway for the OH + $NH_3$ system is qualitatively similar to the one calculated for the OH + $CH_3OH$ reaction (Ocaña et al., 2019), i.e., formation of a H-bonded PRC followed by a transition state with a positive energy barrier. Following that comparison, the observed increase of $k_1$ can be interpreted by the formation of a long-lived PRC at very low temperatures, which surpasses the energy barrier by quantum mechanical tunnelling.

### Effect of $k_1$ in the Abundance of Interstellar $NH_3$

Astrochemical networks apply modified Arrhenius expressions to estimate rate coefficients in a certain temperature interval:

$$k(T) = \alpha\left(\frac{T}{300K}\right)^{\beta} exp^{-\gamma/T} \quad \text{(E4)}$$

For example, KIDA database uses the recommended expression by Atkinson et al. (2004) (**Eq. E3**, where $\beta = 0$) and UDfA database uses the following expression:

$$k_1\,(200 - 3,000K) = 1.47 \times 10^{-13}\left(\frac{T}{300K}\right)^{2.05} exp^{-7\ K/T}\ cm^3 s^{-1} \quad \text{(E5)}$$

Note that these recommended **Eqs E3**, **E5** are valid on the stated temperature range. Using these T-expressions to extrapolate rate coefficients down to 22 K is extremely risky. One gets very low values of $k_1$, on the order of $10^{-27}$ $cm^3\ s^{-1}$ from KIDA expression **Eq. E3** and $10^{-16}$ $cm^3\ s^{-1}$ from UDfA **Eq. E5**, compared with the rate coefficient for the OH + $NH_3$ reaction determined in the present work. Using **Eqs E3** and **E5**, the rate coefficient at 230 K, $k_1$(230 K), and extrapolated $k_1$(200 K) are 6.4 and 8.3 × $10^{-14}$ $cm^3\ s^{-1}$, respectively. At the lowest temperature, the $k_1$(~22 K)/$k_1$(230 K) ratio is around 380. This value means that the rate of formation of $NH_2$ radicals from the reaction of $NH_3$ with OH radicals is really enhanced by more than two orders of magnitude at the typical temperature of a cold dark cloud. Using $k_1$, obtained in this work, and the rate coefficients from the KIDA and UDfA databases, for a typical cold dark cloud, with $H_2$ molecular density of $1 \times 10^4$ $cm^{-3}$ and a temperature of 10 K (close to the one reproduced in this work) (Agúndez and Wakelam, 2013), the change in modelled abundances of $NH_3$ is negligible for both reaction networks. The main destruction route for $NH_3$ in this cold environment is the reaction with $H_3O^+$ cations, being the reaction of $NH_3$ with OH radicals around 1% of that with $H_3O^+$ species.

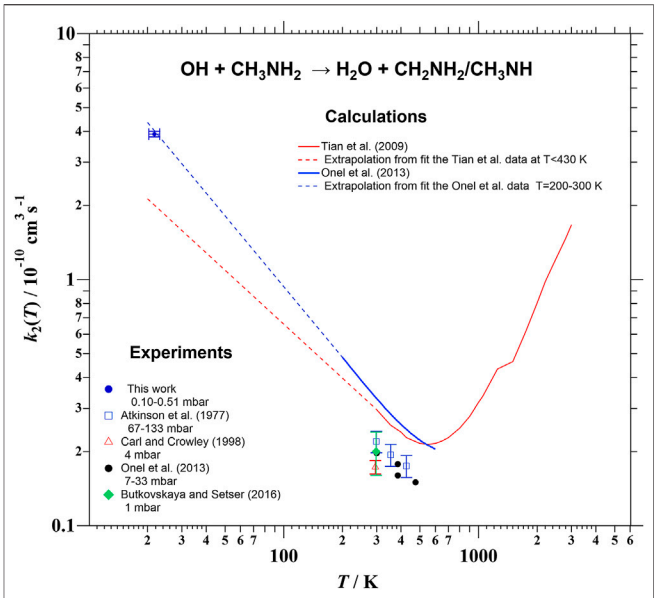


**FIGURE 5 |** Temperature dependence of $k_2$ in the 22–3,000 K range.

## The OH + $CH_3NH_2$ Reaction

### Temperature Dependence of $k_2$

As shown in **Table 1**, no pressure dependence of the rate coefficient for the OH + $CH_3NH_2$ reaction was observed in the investigated range. The resulting $k_2$ at ca. 22 K from the combination of all kinetic data at different gas densities (see **Figure 3B**) is:

$$k_2\,(\sim 22K) = (3.9 \pm 0.1) \times 10^{-10} cm^3 s^{-1}$$

This value together with previously reported $k_2$ over the 298–3,000 K temperature range (Atkinson et al., 1977; Carl and Crowley, 1998; Tian et al., 2009; Onel et al., 2013; Butkovskaya and Setser, 2016) are depicted in **Figure 5**. The temperature dependence of $k_2$ was first measured by Atkinson et al. (1977) at T > 299 K, who reported the following Arrhenius expression:

$$k_2\,(299 - 426\,K) = 1.02 \times 10^{-11} exp^{(455\pm300)\,cal\,mol^{-1}/RT}\ cm^3 s^{-1} \quad \text{(E6)}$$

The activation energy is slightly negative in this case, −0.45 kcal/mol; however more recently, the negative temperature dependence observed experimentally for **Eq. R2** was also reported by Onel et al. (2013) as an expression with

**TABLE 3 |** Summary of the calculated relative (to reactants) energies (in kcal/mol) of the stationary points in the MEP for the OH + $CH_3NH_2$ reaction reported in the literature (see text for more details).

| Channel | PRC | TS | PPC | Products | References |
|---|---|---|---|---|---|
| R2a | — | 0.36 | — | −23.19 | Galano and Alvarez-Idaboy (2008) |
| R2b | — | 0.97 | — | −17.00 | |
| R2a | −0.61 | −0.52 | −28.48 | −23.17 | Tian et al. (2009) |
| R2b | −8.45 | 1.02 | −23.03 | −17.07 | |
| R2a | −6.38 | −1.96 | −29.54 | −43.52 | Onel et al. (2013) |
| R2b | −6.38 | −2.0 | −24.19 | −26.48 | |
| R2a | −5.4 | 1.2 | — | −26.0 | Borduas et al. (2016) |
| R2b | −0.2 | 0.2 | — | −19.0 | |

no activation energy and a T-dependent pre-exponential factor (black circles in **Figure 5**):

$$k_2\,(298-500K) = 1.89\times10^{-11}\left(\frac{T}{298K}\right)^{-0.56} cm^3 s^{-1} \qquad \text{(E7)}$$

Using the experimental Onel's expression, the extrapolated $k_2$(~22 K) is ca. $8\times10^{-11}$ $cm^3\,s^{-1}$ (4.9 times lower than the experimental one reported here), while **Eq. E6** provides an extrapolated $k_2$(~22 K) of $3.4\times10^{-7}$ $cm^3\,s^{-1}$, which is a non-realistic value for a neutral-neutral reaction. Onel et al. (2013) also computed $k_2$ between 200 and 500 K (blue line in **Figure 5**) to be around 60% higher than the experimental values. No experimental kinetic data have been reported at T > 500 K, however Tian et al. (2009) predicted a minimum of $k_2$ around 550 K and a remarkable increase of $k_2$ at higher temperatures, i.e., the rate coefficient for the OH + $CH_3NH_2$ reaction is expected to exhibit a non-Arrhenius behavior. As shown by dashed lines in **Figure 5**, the extrapolated $k_2$ from calculations of Onel et al. (2013) is in excellent agreement with our reported value and the value of $k_2$ obtained by extrapolation of Tian et al. (2009) data is only a factor of ca. 2 lower than the experimental value reported in this work. Additional kinetic studies between 298 and 22 K are clearly needed to confirm the expected trend in the T-dependence of $k_2$.

### Reaction Mechanism

The possible exothermic reaction channels for **Eq. R2** are the H-abstraction from the methyl group (**Eq. R2a**) or from the amino group (**Eq. R2b**):

$$OH + CH_3NH_2 \rightarrow H_2O + CH_2NH_2 \qquad \text{(R2a)}$$
$$\rightarrow H_2O + CH_3NH \qquad \text{(R2b)}$$

Theoretically, the mechanism of **Eq. R2** has been investigated by several groups (Galano and Alvarez-Idaboy, 2008; Tian et al., 2009; Onel et al., 2013; Borduas et al., 2016). The calculations suggest a stepwise mechanism involving the formation of a PRC in the entrance channels (Tian et al., 2009; Onel et al., 2013; Borduas et al., 2016) and a PPC in the exit channels (Tian et al., 2009; Onel et al., 2013). On the other hand, the OH-addition to N and subsequent concerted C-C cleavage, which produces $CH_3$ radicals and $NH_2OH$, is endothermic with an energy barrier of 37.4 kcal/mol (Borduas et al., 2016). For that reason, in **Scheme 2**, the energies of the stationary points along the MEP for the OH + $CH_3NH_2$ reaction is only depicted for the exothermic channels R2a and R2b. The relative energies of PRC, TS, and PPC for reaction pathways R2a and R2c reported in theoretical calculations are summarized in **Table 3** (Galano and Alvarez-Idaboy, 2008; Tian et al., 2009; Onel et al., 2013); Borduas et al., 2016). In the 299–3,000 K temperature range, the dominant exothermic channel is that producing $CH_2NH_2$ radicals (Galano and Alvarez-Idaboy, 2008; Tian et al., 2009). The branching ratio for R2a ($r$) at 298 K was reported to be of 0.797 (Galano and Alvarez-Idaboy, 2008) and 0.74 (Tian et al., 2009). In contrast, Borduas et al. (2016) concluded that channels R2a and R2b are competitive, with energy barriers close to the entrance level energies of the reactants and within 1 kcal $mol^{-1}$ of each other. Nevertheless, the dominance of R2a channel at room temperature has experimentally been confirmed by Nielsen et al. (2011, 2012), Onel et al. (2014), Butkovskaya and Setser (2016). Nielsen et al. (2011, 2012) performed experiments in EUPHORE atmospheric chamber providing a $r$ of (0.75 ± 0.05) for channel R2a. A similar value (0.79 ± 0.15) was found by Onel et al. (2014) and by Butkovskaya and Setser (2016) (0.74 ± 0.05) No measurements or calculations were found at temperatures below room temperature. Thus, further theoretical and/or experimental studies are needed to know what the branching ratios of channels R2a (forming $CH_2NH_2$) and R2b (forming $CH_3NH$) are at interstellar temperatures.

### Effect of $k_2$ in the Abundance of Interstellar $CH_3NH_2$

Neither KIDA database nor UDfA network include this OH-reaction as a potential destruction route for $CH_3NH_2$. However, this reaction is extremely fast at ca. 22 K as it is shown by the experimental rate coefficient for the OH + $CH_3NH_2$ reaction reported here. Our measured $k_2$(~22 K) would, then, lead to a quicker depletion of $CH_3NH_2$ by reaction with OH in astrochemical models. The $k_2$(~22 K)/$k_2$(298 K) ratio is around 20, indicating that the use of $k_2$(298 K) in modelling the ISM would underestimate the loss of $CH_3NH_2$ by OH by more than one order of magnitude. Using the reported $k_2$(~22 K) in the pure gas-phase model from Agúndez and Wakelam (2013), the destruction of $CH_3NH_2$ by OH radicals in a typical cold dark cloud ($H_2$ molecular density of $1\times10^4$ $cm^{-3}$ and temperature 10 K) supposes around 1/3 of that initiated by $HCO^+$ (main depletion route).

## CONCLUSION

The OH-reactivity of $NH_3$ at ca. 22 K is more than two orders of magnitude higher than that observed at the lowest temperature achieved up to now, 230 K. This confirms that the observed curvature in the Arrhenius plot reflects the increase of $k_1$ at low temperatures. Further studies are needed to complete the kinetic

behavior between 22 and 230 K and lower temperatures than 22 K. For $CH_3NH_2$, the determined rate coefficient at ca. 22 K is almost 20 times higher than the one measured at room temperature. The slightly negative temperature dependence of $k_2$ observed by Atkinson et al. (1977) at T > 298 K, implies that the OH-reactivity increases at temperatures lower than room temperature, as observed in this work. These new experimental data indicate that the inclusion of the rate coefficient for the OH + $NH_3$ reaction at 20 K in gas-phase astrochemical models does not significantly change the abundance of $NH_3$ in a typical cold dark cloud since the main destruction route for $NH_3$ is the reaction with $H_3O^+$. However, the inclusion of the rate coefficient for the OH + $CH_3NH_2$ reaction at 20 K, not considered in KIDA and UDfA networks, indicated that the contribution of this destruction route is not negligible, accounting for 1/3 of the main assumed depletion route (reaction with $HCO^+$) in this IS environment with temperature close to 10 K.

## DATA AVAILABILITY STATEMENT

The raw data supporting the conclusion of this article will be made available by the authors, without undue reservation.

## AUTHOR CONTRIBUTIONS

DG performed the experiments, analyzed the kinetic data, and wrote the draft of the article; BB and EJ contributed to the design and supervision of the experiments; AC and EJ participated in the critical revision of the article; JA and EJ got the funds for carrying out this research and managed the projects. All authors discussed the results and contributed to the final manuscript.

## FUNDING

This work has been supported by the Spanish Ministry of Science and Innovation (MICINN) through the CHEMLIFE project (Ref: PID2020-113936GB-I00), the regional government of Castilla-La Mancha through CINEMOL project (Ref: SBPLY/19/180501/000052) and by the University of Castilla-La Mancha—UCLM (Ayudas para la financiación de actividades de investigación dirigidas a grupos (REF: 2020-GRIN-29016 and 2021-GRIN-31279). DG also acknowledges UCLM (Plan Propio de Investigación) for funding his contract during the performance of this investigation.

## ACKNOWLEDGMENTS

The authors acknowledge Francisco J. Maigler for his technical assistance during the performance of these experiments and Dr. Marcelino Agúndez for helpful discussion on the effect of current rate coefficients on the abundance of $NH_3$ and $CH_3NH_2$ in a typical cold dark cloud.

## REFERENCES

Acharyya, K., Herbst, E., Caravan, R. L., Shannon, R. J., Blitz, M. A., and Heard, D. E. (2015). The Importance of OH Radical-Neutral Low Temperature Tunnelling Reactions in Interstellar Clouds Using a New Model. *Mol. Phys.* 113, 2243–2254. doi:10.1080/00268976.2015.1021729

Agúndez, M., and Wakelam, V. (2013). Chemistry of Dark Clouds: Databases, Networks, and Models. *Chem. Rev.* 113, 8710–8737. doi:10.1021/cr4001176

Albaladejo, J., Ballesteros, B., Jiménez, E., Díaz de Mera, Y., and Martínez, E. (2003). Gas-phase OH Radical-Initiated Oxidation of the 3-halopropenes Studied by PLP-LIF in the Temperature Range 228-388 K. *Atmos. Environ.* 37, 2919–2926. doi:10.1016/S1352-2310(03)00297-8

Antiñolo, M., Agúndez, M., Jiménez, E., Ballesteros, B., Canosa, A., Dib, G. E., et al. (2016). Reactivity of OH and $CH_3OH$ between 22 and 64 K: Modeling the Gas Phase Production of $CH_3O$ in Barnard 1b. *ApJ* 823, 25. doi:10.3847/0004-637X/823/1/25

A. Silver, J., and E. Kolb, C. (1980). Rate Constant for the Reaction $NH_3$ + OH → $NH_2$ + $H_2O$ over a Wide Temperature Range. *Chem. Phys. Lett.* 75, 191–195. doi:10.1016/0009-2614(80)80492-1

Atkinson, R., Baulch, D. L., Cox, R. A., Crowley, J. N., Hampson, R. F., Hynes, R. G., et al. (2004). Evaluated Kinetic and Photochemical Data for Atmospheric Chemistry: Part 1 – Gas Phase Reactions of $O_x$, $HO_x$, $NO_x$ and $SO_x$ Species. *Atmos. Chem. Phys.* 4, 1461–1738. doi:10.5194/acpd-3-6179-2003

Atkinson, R., Perry, R. A., and Pitts, J. N. (1977). Rate Constants for the Reaction of the OH Radical with $CH_3SH$ and $CH_3NH_2$ over the Temperature Range 299-426 °K. *J. Chem. Phys.* 66, 1578–1581. doi:10.1063/1.434076

Bada, J. L., and Lazcano, A. (2002). Some like it Hot, but Not the First Biomolecules. *Science* 296, 1982–1983. doi:10.1126/science.1069487

Balucani, N. (2009). Elementary Reactions and Their Role in Gas-phase Prebiotic Chemistry. *Int. J. Mol. Sci.* 10, 2304–2335. doi:10.3390/ijms10052304

Bernstein, M. (2006). Prebiotic Materials from on and off the Early Earth. *Phil. Trans. R. Soc. B* 361, 1689–1702. doi:10.1098/rstb.2006.1913

Blázquez, S., González, D., García-Sáez, A., Antiñolo, M., Bergeat, A., Caralp, F., et al. (2019). Experimental and Theoretical Investigation on the OH + $CH_3C(O)CH_3$ Reaction at Interstellar Temperatures (T = 11.7-64.4 K). *ACS Earth Space Chem.* 3, 1873–1883. doi:10.1021/acsearthspacechem.9b00144

Blázquez, S., González, D., Neeman, E. M., Ballesteros, B., Agúndez, M., Canosa, A., et al. (2020). Gas-phase Kinetics of $CH_3CHO$ with OH Radicals between 11.7 and 177.5 K. *Phys. Chem. Chem. Phys.* 22, 20562–20572. doi:10.1039/D0CP03203D

Bocherel, P., Herbert, L. B., Rowe, B. R., Sims, I. R., Smith, I. W. M., and Travers, D. (1996). Ultralow-Temperature Kinetics of CH($X^2\Pi$) Reactions: Rate Coefficients for Reactions with $O_2$ and NO (T = 13–708 K), and with $NH_3$ (T = 23–295 K). *J. Phys. Chem.* 100, 3063–3069. doi:10.1021/jp952628f

Borduas, N., Abbatt, J. P. D., Murphy, J. G., So, S., and Da Silva, G. (2016). Gas-Phase Mechanisms of the Reactions of Reduced Organic Nitrogen Compounds with OH Radicals. *Environ. Sci. Technol.* 50, 11723–11734. doi:10.1021/acs.est.6b03797

Bourgalais, J., Capron, M., Kailasanathan, R. K. A., Osborn, D. L., Hickson, K. M., Loison, J.-C., et al. (2015). The C($^3$P) + $NH_3$ Reaction in Interstellar Chemistry. I. Investigation of the Product Formation Channels. *ApJ* 812, 106–140. doi:10.1088/0004-637X/812/2/106

Bowdridge, M., Furue, H., and Pacey, P. D. (1996). Properties of Transition Species in the Reactions of Hydroxyl with Ammonia and with Itself. *J. Phys. Chem.* 100, 1676–1681. doi:10.1021/jp9522573

Butkovskaya, N. I., and Setser, D. W. (2016). Branching Ratios and Vibrational Distributions in Water-Forming Reactions of OH and OD Radicals with Methylamines. *J. Phys. Chem. A.* 120, 6698–6711. doi:10.1021/acs.jpca.6b06411

Canosa, A., Ocaña, A. J., Antiñolo, M., Ballesteros, B., Jiménez, E., and Albaladejo, J. (2016). Design and testing of temperature tunable de Laval nozzles for applications in gas-phase reaction kinetics. *Exp. Fluids* 57. doi:10.1007/s00348-016-2238-1

Carl, S. A., and Crowley, J. N. (1998). Sequential Two (Blue) Photon Absorption by NO2 in the Presence of H2 as a Source of OH in Pulsed Photolysis Kinetic Studies: Rate Constants for Reaction of OH with $CH_3NH_2$, $(CH_3)_2NH$, $(CH_3)_3N$, and $C_2H_5NH_2$ at 295 K. *J. Phys. Chem. A.* 102, 8131–8141. doi:10.1021/jp9821937

Cazaux, S., Cobut, V., Marseille, M., Spaans, M., and Caselli, P. (2010). Water Formation on Bare Grains: When the Chemistry on Dust Impacts Interstellar Gas. *A&A* 522, A74. doi:10.1051/0004-6361/201014026

Cheung, A. C., Rank, D. M., Townes, C. H., Thornton, D. D., and Welch, W. J. (1968). Detection of NH3Molecules in the Interstellar Medium by Their Microwave Emission. *Phys. Rev. Lett.* 21, 1701–1705. doi:10.1103/PhysRevLett.21.1701

Chyba, C., and Sagan, C. (1992). Endogenous Production, Exogenous Delivery and Impact-Shock Synthesis of Organic Molecules: an Inventory for the Origins of Life. *Nature* 355, 125–132. doi:10.1038/355125a0

Cleaves, H. J., Chalmers, J. H., Lazcano, A., Miller, S. L., and Bada, J. L. (2008). A Reassessment of Prebiotic Organic Synthesis in Neutral Planetary Atmospheres. *Orig. Life Evol. Biosph.* 38, 105–115. doi:10.1007/s11084-007-9120-3

Corchado, J. C., Espinosa-Garcia, J., Hu, W.-P., Rossi, I., and Truhlar, D. G. (1995). Dual-Level Reaction-Path Dynamics (The ///Approach to VTST with Semiclassical Tunneling). Application to OH + $NH_3$ → $H_3O$ + $NH_2$. *J. Phys. Chem.* 99, 687–694. doi:10.1021/j100002a037

Diau, E. W. G., Tso, T. L., and Lee, Y. P. (1990). Kinetics of the Reaction Hydroxyl + Ammonia in the Range 273-433 K. *J. Phys. Chem.* 94, 5261–5265. doi:10.1021/j100376a018

Ehrenfreund, P., Irvine, W., Becker, L., Blank, J., Brucato, J. R., Colangeli, L., et al. (2002). Astrophysical and Astrochemical Insights into the Origin of Life. *Rep. Prog. Phys.* 65, 1427–1487. doi:10.1088/0034-4885/65/10/202

Espinosa-García, J., and Corchado, J. C. (1994). Analysis of Certain Factors in the Direct Dynamics Method: Variational Rate Constant of the $NH_3$+OH→$NH_2$+$H_2O$ Reaction. *J. Chem. Phys.* 101, 8700–8708. doi:10.1063/1.468065

Förstel, M., Bergantini, A., Maksyutenko, P., Góbi, S., and Kaiser, R. I. (2017). Formation of Methylamine and Ethylamine in Extraterrestrial Ices and Their Role as Fundamental Building Blocks of Proteinogenicα-Amino Acids. *ApJ* 845, 83. doi:10.3847/1538-4357/aa7edd

Fourikis, N., Takagi, K., and Morimoto, M. (1974). Detection of Interstellar Methylamine by its 2_{02}->1_{10} A_{a̋-}} State Transition. *ApJ* 191, L139. doi:10.1086/181570

Freeman, A., and Millar, T. J. (1983). Formation of Complex Molecules in TMC-1. *Nature* 301, 402–404. doi:10.1038/301402a0

Fujii, N., Chiba, K., Uchida, S., and Miyama, H. (1986). The Rate Constants of the Elementary Reactions of $NH_3$ with O and OH. *Chem. Phys. Lett.* 127, 141–144. doi:10.1016/S0009-2614(86)80243-3

Fujii, N., Miyama, H., and Asaba, T. (1981). Determination of the Rate Constant for the Reaction $NH_3$ + OH → $NH_2$ + $H_2O$. *Chem. Phys. Lett.* 80, 355–357. doi:10.1016/0009-2614(81)80125-X

Galano, A., and Alvarez-Idaboy, J. R. (2008). Branching Ratios of Aliphatic Amines + OH Gas-phase Reactions: A Variational Transition-State Theory Study. *J. Chem. Theor. Comput.* 4, 322–327. doi:10.1021/ct7002786

Garrod, R. T. (2013). A Three-phase Chemical Model of Hot Cores: The Formation of Glycine. *ApJ* 765, 60. doi:10.1088/0004-637X/765/1/60

Garrod, R. T., Weaver, S. L. W., and Herbst, E. (2008). Complex Chemistry in Star-forming Regions: An Expanded Gas-Grain Warm-up Chemical Model. *ApJ* 682, 283–302. doi:10.1086/588035

Gerin, M., Neufeld, D. A., and Goicoechea, J. R. (2016). Interstellar Hydrides. *Annu. Rev. Astron. Astrophys.* 54, 181–225. doi:10.1146/annurev-astro-081915-023409

Gianturco, F. A., Yurtsever, E., Satta, M., and Wester, R. (2019). Modeling Ionic Reactions at Interstellar Temperatures: The Case of $NH_2$- + $H_2$ ⇔ $NH_3$ + H-. *J. Phys. Chem. A.* 123, 9905–9918. doi:10.1021/acs.jpca.9b07317

Giménez, X., Moreno, M., and Lluch, J. M. (1992). Ab Initio study of the NH3 + OH Reaction. *Chem. Phys.* 165, 41–46. doi:10.1016/0301-0104(92)80041-S

Goicoechea, J. R., Joblin, C., Contursi, A., Berné, O., Cernicharo, J., Gerin, M., et al. (2011). OH Emission from Warm and Dense Gas in the Orion Bar PDR. *A&A* 530, L16. doi:10.1051/0004-6361/201116977

Hack, W., Hoyerman, K., and Wagner, H. G. (1974). Reaktionen des Hydroxylradikals mit Ammoniak und Hydrazin in der Gasphase. *Ber.Bunsenges. Phys. Chem. Chem. Phys.* 78, 386–391.

Halfen, D. T., Ilyushin, V. V., and Ziurys, L. M. (2013). Insights into Surface Hydrogenation in the Interstellar Medium: Observations of Methanimine and Methyl Amine in Sgr B2(N). *ApJ* 767, 66. doi:10.1088/0004-637X/767/1/66

Heard, D. E. (2018). Rapid Acceleration of Hydrogen Atom Abstraction Reactions of OH at Very Low Temperatures through Weakly Bound Complexes and Tunneling. *Acc. Chem. Res.* 51, 2620–2627. doi:10.1021/acs.accounts.8b00304

Herbst, E., and Klemperer, W. (1973). The Formation and Depletion of Molecules in Dense Interstellar Clouds. *ApJ* 185, 505–533. doi:10.1086/152436

Herbst, E. (1985). The Rate of the Radiative Association Reaction between $CH_3$(+) and $NH_3$ and its Implications for Interstellar Chemistry. *ApJ* 292, 484–486. doi:10.1086/163179

Herbst, E., and van Dishoeck, E. F. (2009). Complex Organic Interstellar Molecules. *Annu. Rev. Astron. Astrophys.* 47, 427–480. doi:10.1146/annurev-astro-082708-101654

Hickson, K. M., Loison, J.-C., Bourgalais, J., Capron, M., Picard, S. D. L., Goulay, F., et al. (2015). The C($^3$P) + $NH_3$ Reaction in Interstellar Chemistry. Ii. Low Temperature Rate Constants and Modeling of Nh, $Nh_2$, and $Nh_3$Abundances in Dense Interstellar Clouds. *ApJ* 812, 107–125. doi:10.1088/0004-637X/812/2/107

Ioppolo, S., Fedoseev, G., Chuang, K.-J., Cuppen, H. M., Clements, A. R., Jin, M., et al. (2021). A Non-energetic Mechanism for glycine Formation in the Interstellar Medium. *Nat. Astron.* 5, 197–205. doi:10.1038/s41550-020-01249-0

Jeffries, J. B., and Smith, G. P. (1986). Kinetics of the Reaction Hydroxyl + Ammonia. *J. Phys. Chem.* 90, 487–491. doi:10.1021/j100275a027

Jiménez, E., Antiñolo, M., Ballesteros, B., Canosa, A., and Albaladejo, J. (2016). First Evidence of the Dramatic Enhancement of the Reactivity of Methyl Formate ($HC(O)OCH_3$) with OH at Temperatures of the Interstellar Medium: a Gas-phase Kinetic Study between 22 K and 64 K. *Phys. Chem. Chem. Phys.* 18, 2183–2191. doi:10.1039/C5CP06369H

Jiménez, E., Ballesteros, B., Canosa, A., Townsend, T. M., Maigler, F. J., Napal, V., et al. (2015). Development of a Pulsed Uniform Supersonic Gas Expansion System Based on an Aerodynamic Chopper for Gas Phase Reaction Kinetic Studies at Ultra-low Temperatures. *Rev. Scientific Instr.* 86, 045108. doi:10.1063/1.4918529

Jiménez, E., Lanza, B., Garzón, A., Ballesteros, B., and Albaladejo, J. (2005). Atmospheric Degradation of 2-butanol, 2-Methyl-2-Butanol, and 2,3-Dimethyl-2-Butanol: OH Kinetics and UV Absorption Cross Sections. *J. Phys. Chem. A.* 109, 10903–10909. doi:10.1021/jp054094g

Jonusas, M., Leroux, K., and Krim, L. (2020). N + H Surface Reaction under Interstellar Conditions: Does the $NH/NH_2/NH_3$ Distribution Depend on N/H Ratio? *J. Mol. Struct.* 1220, 128736. doi:10.1016/j.molstruc.2020.128736

Kaifu, N., Morimoto, M., Nagane, K., Akabane, K., Iguchi, T., and Takagi, K. (1974). Detection of Interstellar Methylamine. *ApJ* 191, L135. doi:10.1086/181569

Kim, Y. S., and Kaiser, R. I. (2011). On the Formation of Amines ($RNH_2$) and the Cyanide Anion ($C_n^-$) in Electron-Irradiated Ammonia-Hydrocarbon Interstellar Model Ices. *ApJ* 729, 68. doi:10.1088/0004-637X/729/1/68

Kurylo, M. J. (1973). Kinetics of the Reactions OH (V = O) + $NH_3$ →; $H_2O$ + $NH_2$ and OH(v = O) + $O_3$ → $HO_2$ + $O_2$ at 298°K. *Chem. Phys. Lett.* 23, 467–471. doi:10.1016/0009-2614(73)89003-7

Linnartz, H., Ioppolo, S., and Fedoseev, G. (2015). Atom Addition Reactions in Interstellar Ice Analogues. *Int. Rev. Phys. Chem.* 34, 205–237. doi:10.1080/0144235X.2015.1046679

Lynch, B. J., Fast, P. L., Harris, M., and Truhlar, D. G. (2000). Adiabatic Connection for Kinetics. *J. Phys. Chem. A.* 104, 4811–4815. doi:10.1021/jp000497z

Miller, S. L. (1953). A Production of Amino Acids under Possible Primitive Earth Conditions. *Science* 117, 528–529. doi:10.1126/science.117.3046.528

Monge-Palacios, M., Corchado, J. C., and Espinosa-Garcia, J. (2013a). Dynamics Study of the OH + $NH_3$ Hydrogen Abstraction Reaction Using QCT Calculations Based on an Analytical Potential Energy Surface. *J. Chem. Phys.* 138, 214306–214312. doi:10.1063/1.4808109

Monge-Palacios, M., and Espinosa-Garcia, J. (2013). Role of Vibrational and Translational Energy in the OH + $NH_3$ Reaction: A Quasi-Classical Trajectory Study. *J. Phys. Chem. A.* 117, 5042–5051. doi:10.1021/jp403571y

Monge-Palacios, M., Rangel, C., and Espinosa-Garcia, J. (2013b). Ab Initiobased Potential Energy Surface and Kinetics Study of the OH + $NH_3$ hydrogen Abstraction Reaction. *J. Chem. Phys.* 138, 084305. doi:10.1063/1.4792719

Neeman, E. M., González, D., Blázquez, S., Ballesteros, B., Canosa, A., Antiñolo, M., et al. (2021). The Impact of Water Vapor on the OH Reactivity toward

$CH_3CHO$ at Ultra-low Temperatures (21.7-135.0 K): Experiments and Theory. *J. Chem. Phys.* 155, 034306. doi:10.1063/5.0054859

Nguyen, T. L., and Stanton, J. F. (2017). High-level Theoretical Study of the Reaction between Hydroxyl and Ammonia: Accurate Rate Constants from 200 to 2500 K. *J. Chem. Phys.* 147, 152704. doi:10.1063/1.4986151

Nielsen, C., D'Anna, B., Aursnes, M., and Boreave, A. (2012). *Summary Report from Atmospheric Chemistry Studies of Amines, Nitrosamines, Nitramines and Amides; Climit Project No. 208122*. Oslo: NILU, University of Oslo.

Nielsen, C. J., D'Anna, B., Karl, M., Aursnes, M., Boreave, A., Bossi, R., et al. (2011). *Summary Report: Photo-Oxidation of Methylamine, Dimethylamine and Trimetahylamine. Climit Project No. 201604NILU 2*. Oslo: University of Oslo.

Nizamov, B., and Leone, S. R. (2004). Rate Coefficients and Kinetic Isotope Effect for the $C_2H$ Reactions with $NH_3$ and $ND_3$ in the 104–294 K Temperature Range. *J. Phys. Chem. A.* 108, 3766–3771. doi:10.1021/jp031361e

Nyman, G. (1996). Quantum Scattering Calculations on the $NH_3$+OH→$NH_2$+$H_2O$ Reaction. *J. Chem. Phys.* 104, 6154–6167. doi:10.1063/1.471281

Ocaña, A. J., Blázquez, S., Ballesteros, B., Canosa, A., Antiñolo, M., Albaladejo, J., et al. (2018). Gas Phase Kinetics of the OH + $CH_3CH_2OH$ Reaction at Temperatures of the Interstellar Medium (T = 21-107 K). *Phys. Chem. Chem. Phys.* 20, 5865–5873. doi:10.1039/C7CP07868D

Ocaña, A. J., Blázquez, S., Potapov, A., Ballesteros, B., Canosa, A., Antiñolo, M., et al. (2019). Gas-phase Reactivity of $CH_3OH$ toward OH at Interstellar Temperatures (11.7-177.5 K): Experimental and Theoretical Study. *Phys. Chem. Chem. Phys.* 21, 6942–6957. doi:10.1039/c9cp00439d

Ocaña, A. J., Jiménez, E., Ballesteros, B., Canosa, A., Antiñolo, M., Albaladejo, J., et al. (2017). Is the Gas-phase OH+$H_2CO$ Reaction a Source of HCO in Interstellar Cold Dark Clouds? A Kinetic, Dynamic, and Modeling Study. *ApJ* 850, 28. doi:10.3847/1538-4357/aa93d9

Ohishi, M., Suzuki, T., Hirota, T., Saito, M., and Kaifu, N. (2019). Detection of a New Methylamine ($CH_3NH_2$) Source: Candidate for Future glycine Surveys. *Publ. Astron. Soc. Jpn.* 71, 1–11. doi:10.1093/pasj/psz068

Onel, L., Blitz, M., Dryden, M., Thonger, L., and Seakins, P. (2014). Branching Ratios in Reactions of OH Radicals with Methylamine, Dimethylamine, and Ethylamine. *Environ. Sci. Technol.* 48, 9935–9942. doi:10.1021/es502398r

Onel, L., Thonger, L., Blitz, M. A., Seakins, P. W., Bunkan, A. J. C., Solimannejad, M., et al. (2013). Gas-phase Reactions of OH with Methyl Amines in the Presence or Absence of Molecular Oxygen. An Experimental and Theoretical Study. *J. Phys. Chem. A.* 117, 10736–10745. doi:10.1021/jp406522z

Perry, R. A., Atkinson, R., and Pitts, j. N., Jr (1976). Rate Constants for the Reactions OH+$H_2S$→$H_2O$+SH and OH+$NH_3$→$H_2O$+$NH_2$ over the Temperature Range 297-427 °K. *J. Chem. Phys.* 64, 3237. doi:10.1063/1.432663

Potapov, A., Canosa, A., Jiménez, E., and Rowe, B. (2017). Uniform Supersonic Chemical Reactors: 30 Years of Astrochemical History and Future Challenges. *Angew. Chem. Int. Ed.* 56, 8618–8640. doi:10.1002/anie.201611240

Rednyk, S., RoučkaKovalenko, Š., Kovalenko, A., Tran, T. D., Dohnal, P., Plašil, R., et al. (2019). Reaction of $NH^+$, $NH_2^+$, and $NH_3^+$ Ions with $H_2$ at Low Temperatures. *A&A* 625, A74–A78. doi:10.1051/0004-6361/201834149

Salimian, S., Hanson, R. K., and Kruger, C. H. (1984). High Temperature Study of the Reactions of O and OH with $NH_3$. *Int. J. Chem. Kinet.* 16, 725–739. doi:10.1002/kin.550160609

Sandford, S. A., Nuevo, M., Bera, P. P., and Lee, T. J. (2020). Prebiotic Astrochemistry and the Formation of Molecules of Astrobiological Interest in Interstellar Clouds and Protostellar Disks. *Chem. Rev.* 120, 4616–4659. doi:10.1021/acs.chemrev.9b00560

Scott, G. B. I., Freeman, C. G., and McEwan, M. J. (1997). The Interstellar Synthesis of Ammonia. *Monthly Notices R. Astronomical Soc.* 290, 636–638. doi:10.1093/mnras/290.4.636

Sims, I. R., Queffelec, J. L., Defrance, A., Rebrion-Rowe, C., Travers, D., Bocherel, P., et al. (1994). Ultralow Temperature Kinetics of Neutral-Neutral Reactions. The Technique and Results for the Reactions CN+$O_2$down to 13 K and CN+$NH_3$down to 25 K. *J. Chem. Phys.* 100, 4229–4241. doi:10.1063/1.467227

Sleiman, C., El Dib, G., Rosi, M., Skouteris, D., Balucani, N., and Canosa, A. (2018a). Low Temperature Kinetics and Theoretical Studies of the Reaction CN + $CH_3NH_2$: a Potential Source of Cyanamide and Methyl Cyanamide in the Interstellar Medium. *Phys. Chem. Chem. Phys.* 20, 5478–5489. doi:10.1039/c7cp05746f

Sleiman, C., El Dib, G., Talbi, D., and Canosa, A. (2018b). Gas Phase Reactivity of the CN Radical with Methyl Amines at Low Temperatures (23-297 K): A Combined Experimental and Theoretical Investigation. *ACS Earth Space Chem.* 2, 1047–1057. doi:10.1021/acsearthspacechem.8b00098

Smith, I. W. M., and Barnes, P. W. (2013). Advances in Low Temperature Gas-phase Kinetics. *Annu. Rep. Prog. Chem. Sect. C: Phys. Chem.* 109, 140–166. doi:10.1039/c3pc90011h

Sorrell, W. H. (2001). Origin of Amino Acids and Organic Sugars in Interstellar Clouds. *Astrophys. J.* 555, L129–L132. doi:10.1086/322525

Stephens, R. D. (1984). Absolute Rate Constants for the Reaction of Hydroxyl Radicals with Ammonia from 297 to 364 K. *J. Phys. Chem.* 88, 3308–3313. doi:10.1021/j150659a034

Stuhl, F. (1973). Absolute Rate Constant for the Reaction OH+$NH_3$→$NH_2$+$H_2O$. *J. Chem. Phys.* 59, 635–637. doi:10.1063/1.1680069

Taylor, S. E., Goddard, A., Blitz, M. A., Cleary, P. A., and Heard, D. E. (2008). Pulsed Laval Nozzle Study of the Kinetics of OH with Unsaturated Hydrocarbons at Very Low Temperatures. *Phys. Chem. Chem. Phys.* 10, 422–437. doi:10.1039/B711411G

Theule, P., Borget, F., Mispelaer, F., Danger, G., Duvernay, F., Guillemin, J. C., et al. (2011). Hydrogenation of Solid Hydrogen Cyanide HCN and Methanimine $CH_2NH$ at Low Temperature. *Astron. Astrophys.* 534, A64. doi:10.1051/0004-6361/201117494

Tian, W., Wang, W., Zhang, Y., and Wang, W. (2009). Direct Dynamics Study on the Mechanism and the Kinetics of the Reaction of $CH_3NH_2$ with OH. *Int. J. Quan. Chem.* 109, 1566–1575. doi:10.1002/qua.22000

Vahedpour, M., Douroudgari, H., Afshar, S., and Asgharzade, S. (2018). Comparison of Atmospheric Reactions of $NH_3$ and $NH_2$ with Hydroxyl Radical on the Singlet, Doublet and Triplet Potential Energy Surfaces, Kinetic and Mechanistic Study. *Chem. Phys.* 507, 51–69. doi:10.1016/j.chemphys.2018.03.022

van Dishoeck, E. F., Jansen, D. J., Schilke, P., and Phillips, T. G. (1993). Detection of the Interstellar $NH_2$ Radical. *Astrophys. J.* 416, L83. doi:10.1086/187076

Weinreb, S., Barret, A. H., Meeks, M. L., and Henry, J. C. (1963). Radio Observations of OH in the Interstellar Medium. *Nature* 200, 829–831. doi:10.1038/200829a0

Wilson, T. L., Gaume, R. A., and Johnston, K. J. (1993). Ammonia in the $W_3$(OH) Region. *Astrophys. J.* 402, 230. doi:10.1086/172126

Woon, D. E. (2021). A Continously Updated List of the Observed Molecules Is. available online: http://www.astrochymist.org.

Woon, D. E. (2002). Pathways to Glycine and Other Amino Acids in Ultraviolet-Irradiated Astrophysical Ices Determined via Quantum Chemical Modeling. *Astrophys. J.* 571, L177–L180. doi:10.1086/341227

Zabielski, M. F., and Seery, D. J. (1985). High Temperature Measurements of the Rate of the Reaction of OH with $NH_3$. *Int. J. Chem. Kinet.* 17, 1191–1199. doi:10.1002/kin.550171105

Zellner, R., and Smith, I. W. M. (1974). Rate Constants for the Reactions of OH with $NH_3$ and $HNO_3$. *Chem. Phys. Lett.* 26, 72–74. doi:10.1016/0009-2614(74)89086-X

**Conflict of Interest:** The authors declare that the research was conducted in the absence of any commercial or financial relationships that could be construed as a potential conflict of interest.

**Publisher's Note:** All claims expressed in this article are solely those of the authors and do not necessarily represent those of their affiliated organizations, or those of the publisher, the editors and the reviewers. Any product that may be evaluated in this article, or claim that may be made by its manufacturer, is not guaranteed or endorsed by the publisher.